J. Phys. D: Appl. Phys. **31** (1998) L25–L30. Printed in the UK PII: S0022-3727(98)90251-0

RAPID COMMUNICATION

Separation of submicrometre particles using a combination of dielectrophoretic and electrohydrodynamic forces

N G Green and H Morgan

Bioelectronics Research Centre,
Department of Electronics and Electrical Engineering, Rankine Building,
Oakfield Avenue, University of Glasgow, Glasgow G12 8LT, UK

Received 30 December 1997

Abstract. The controlled spatial separation of submicrometre particles by a combination of dielectrophoretic and electrohydrodynamic forces is demonstrated for the first time. Using planar microelectrode arrays, a mixture of two differently sized particles (93 nm and 216 nm diameter latex spheres) has been separated into constituent components. The particles separate into distinct bands, spatially separated from each other. The separation pattern is reproduced across an entire electrode array, indicating that the method could be used as a means of rapid nanoparticle separation, positioning and processing.

In spatially non-uniform ac electric fields, dielectric particles move as a consequence of the interaction of the dipole induced in the particle and the applied field gradient. This movement was termed dielectrophoresis (DEP) by Pohl [1]. In the years subsequent to Pohl's early pioneering work, this developed into a successful technology for the manipulation, characterization and separation of cells and micro-organisms [2, 3]. More recently, through the use of advanced microelectrode fabrication techniques, the technology has moved into the submicrometre world so that particles such as latex spheres, macromolecules, DNA and viruses can now be characterized and separated [4–10]. The DEP force depends (amongst other things) on the particle volume, therefore high electric field gradients are required to move submicrometre particles. As a consequence of electrohydrodynamic (EHD) effects, the high fields gives rise to fluid movement and this fluid movement can cause particle movement through the viscous drag force.

The total force on a polarizable particle in a non-uniform a.c. field can be written as the sum of a number of independently acting forces:

$$\bar{F}_{\text{Total}} = \bar{F}_{\text{DEP}} + \bar{F}_{\text{Viscous}} + \bar{F}_{\text{Other}}. \tag{1}$$

Apart from the DEP force and the viscous force the other forces in this equation include sedimentation and thermal randomizing forces (which drive diffusion when it occurs). For particles of diameter less than 1 μm, thermal effects can dominate, but as has been demonstrated previously [4–10] the DEP force can be sufficient to produce deterministic particle movement. The dielectrophoretic force can be written as

$$\bar{F}_{\text{DEP}} = \text{Re}\{(\bar{m}(\omega) \cdot \nabla)\bar{E}\} \tag{2}$$

where $\bar{E}$ is the electric field, $\bar{m}(\omega)$ is the induced dipole moment of the particle and Re{ } indicates the real part of. For a homogeneous dielectric sphere, the induced dipole moment is given by

$$\bar{m}(\omega) = 4\pi\varepsilon_m a^3 K(\omega)\bar{E} \tag{3}$$

where ω is the angular field frequency, a the particle radius and $K(\omega)$ the Clausius–Mossotti factor given by

$$K(\omega) = \frac{\varepsilon_p^* - \varepsilon_m^*}{\varepsilon_p^* + 2\varepsilon_m^*} \tag{4}$$

where ε_p^* and ε_m^* are the complex permittivities of the particle and the medium respectively. The complex permittivity is $\varepsilon^* = \varepsilon - \text{j}\sigma/\omega$, where $\text{j} = \sqrt{-1}$, ε is the permittivity and σ is the conductivity of the dielectric. The time averaged DEP force is found by substituting equation (3) into (2) and is given by

$$\langle \bar{F}_{\text{DEP}} \rangle = 2\pi\varepsilon_m a^3 \,\text{Re}\{K(\omega)\}\nabla|E_{\text{rms}}|^2 \tag{5}$$

where $\nabla|E_{\text{rms}}|^2$ is the gradient of the square of the rms electric field. The Clausius–Mossotti factor not only depends on the dielectric properties of the particle and

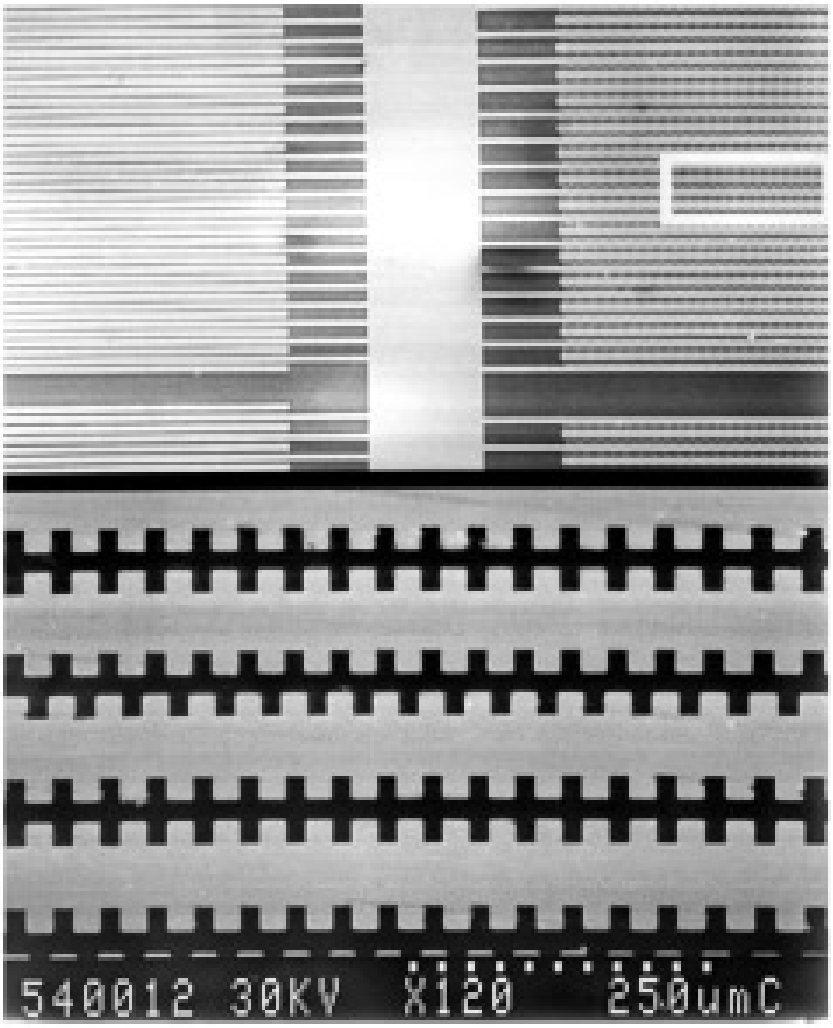

Figure 1. Scanning electron micrograph of a castellated microelectrode used for separation experiments. The electrode was manufactured using direct-write electron-beam lithography and the feature size and electrode gap is 4 μm.

medium, but also on the frequency of the applied field. The variation in this factor results in a frequency-dependent dielectrophoretic force that is unique to a particular particle type. As a consequence dielectrophoresis can be used as an effective means of separating particles, solely according to their dielectric properties and size.

For a spherical particle in a fluid of viscosity η, the viscous drag term in equation (1) is given by Stoke's law

$$\bar{F}_{\text{viscous}} = 6\pi\eta a\bar{v} \tag{6}$$

where $\bar{v}$ is the velocity of the particle. Under the influence of an electric field, heat is generated in the medium, resulting in local temperature gradients which in turn give rise to gradients in the conductivity and permittivity of the medium. These gradients can induce fluid movement, and experiments show that for a given set of parameters (applied voltage, medium conductivity, frequency, electrode geometry etc) the resulting fluid flow has a reproducible pattern [11]. As a consequence the drag force exerted by the moving fluid must be considered in the total force expression (equation (1)). In this communication we demonstrate the manner in which electrohydrodynamic and dielectrophoretic forces can be combined and used as a means of separating particles.

Experiments were performed using planar gold electrodes fabricated on glass or quartz substrates by direct write electron-beam lithography. In brief, the electrode pattern was written onto mask plates (Hoya Corporation) using electron beam lithography (Leica EBPG HR5 beamwriter). After development, a gold layer was evaporated over the patterned resist and lift-off was performed in acetone to remove excess resist and gold. The remaining chrome underlayer was then removed using a chemical wet etch.

The finished electrodes were 25×25 mm in size with an active area covering a few hundred mm^2. An SEM of part of the electrode array used in this work is shown in figure 1 and the dimensions of the electrodes were 4 μm between opposite and nearest neighbour castellations. In order to be able to generate high electric field gradients, accurate feature definition of the order of 100 nm or less

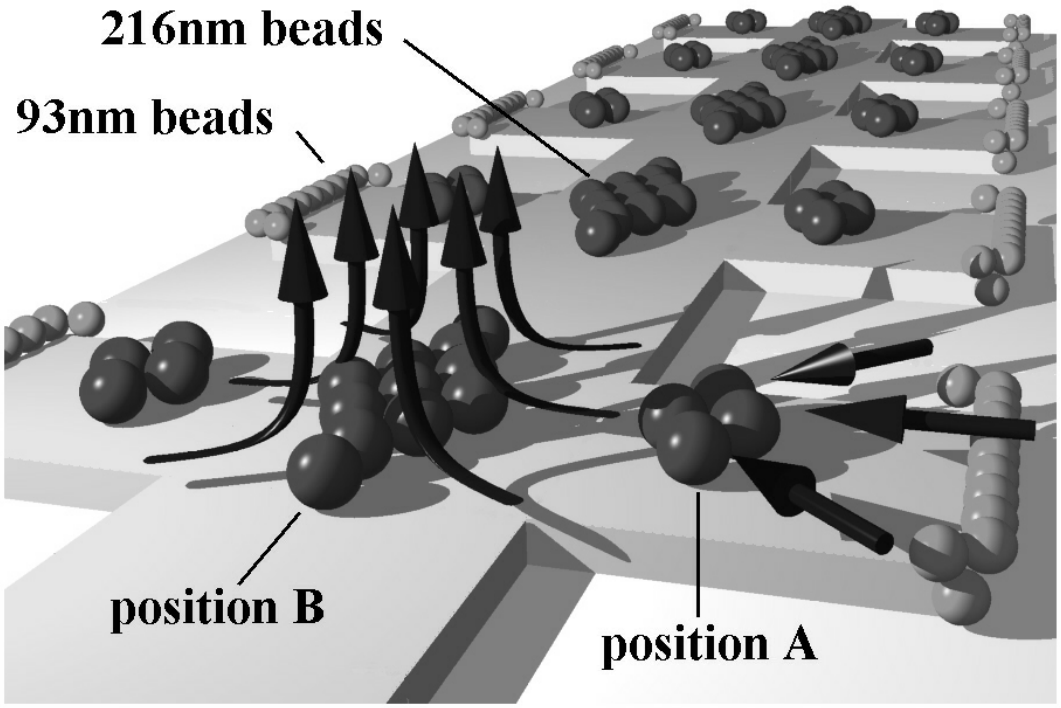

Figure 2. Schematic illustration of the fluid flow patterns observed on the microelectrodes at frequencies below 500 kHz. Fluid moves in from the electrode edges and the flow lines run parallel to the substrate. At the centre of the electrode the converging flows move upwards, perpendicular to the substrate. Spheres that are not held by dielectrophoretic forces experience a viscous drag and are pushed into the centre where they settle at the stagnation point.

is required and electron-beam lithography must be used. The electric field patterns for these electrodes have been published elsewhere [10].

The particles used in the experiments were carboxylate modified latex spheres (Molecular Probes, Eugene, Oregon). The spheres had a net negative charge and were supplied preloaded with a fluorescent dye. The suspending medium was 1 mM potassium chloride and experiments were recorded using fluorescence microscopy (Nikon Microphot) and a video recording/capture system.

A sample consisting of a 1:1 mixture of yellow-green (FITC) 93 nm diameter spheres and red (Nile red) 216 nm diameter spheres suspended in 1 mM KCl (conductivity 15 mS m^{-1}) was prepared and pipetted onto the electrode array. An a.c. signal was applied to the electrode and varied in the ranges 100 Hz to 20 MHz and 0 to 20 V peak to peak.

At frequencies greater than 500 kHz, the particles behaved in a manner consistent with conventional dielectrophoretic theory. Particles experienced either positive or negative forces depending on whether the particles were more or less polarizable than the medium [12]. At the conductivity used in these experiments the DEP force changed from + to − at a frequency of 20 MHz for the 93 nm beads and at a frequency in the range 2 to 3 MHz for the 216 nm beads. At 500 kHz, both the 93 nm and 216 nm spheres experienced positive dielectrophoresis. However, as the frequency was decreased below this point both particles continued to experience positive DEP, but below 500 kHz fluid flow became more apparent. It was observed that, at any given frequency, increasing the potential increased the velocity of the fluid (measured indirectly by observing the movement of the spheres). The movement of the fluid exerted a viscous drag on the particles and at a certain threshold fluid velocity it was observed that the particles moved with the fluid flow in a direction that drove them onto the electrode surface and away from the electrode edge. For frequencies below 500 kHz the direction of the flow was constant, parallel to the substrate surface and perpendicular to the edge of the electrodes. This flow pattern is shown schematically in figure 2.

At a frequency of 100 kHz and a potential difference of 1 V peak to peak, all the particles collected at the high field points on the electrodes under the influence of positive dielectrophoresis. Increasing the potential to a voltage of 8 V peak to peak produced an increase in the fluid movement and as a result the 216 nm diameter spheres moved in towards the central region of the metal. The particles moved a certain fixed distance from the edge and this distance depended on the applied potential: presumably the particles moved to a region where the positive dielectrophoretic force and the viscous drag force balanced each other. This is represented by position A in figure 2. For a constant applied potential, the particles were observed to remain at this equilibrium point indefinitely. Reducing the potential resulted in a reduction in the fluid velocity so that the spheres moved back to the high field points at the edges of the electrodes under DEP forces.

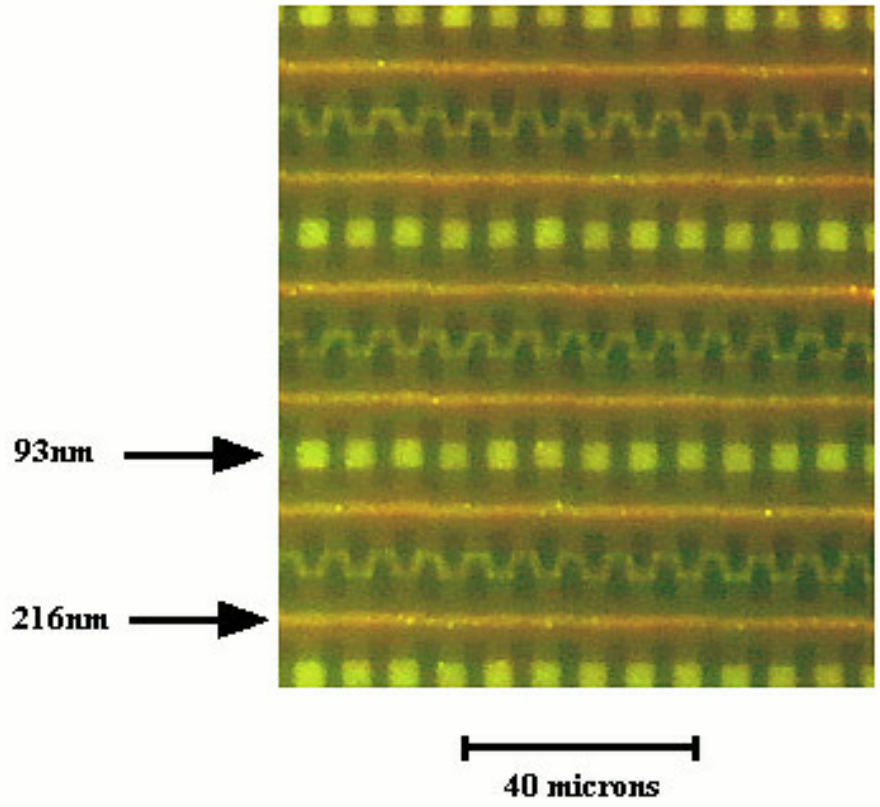

Figure 3. Fluorescence video image showing the separation of red 216 nm and yellow-green 93 nm latex spheres under the influence of combined DEP and EHD forces in the microelectrode array shown in figure 1. The larger spheres move into the centre of the electrode and form long continuous ribbons at the field minimum, while the smaller spheres remain trapped at the electrode tips under positive DEP. This image also shows the 93 nm spheres forming long pearl-chains extending from one electrode to the opposite neighbour. (Note that this figure can be seen in colour on the web.)

(This figure can be viewed in colour in the electronic version of the article; see http://www.iop.org)

At a frequency of 100 kHz and a potential of between 10 and 15 V peak to peak, the fluid streams from opposite edges of the same electrode converged. As a result the 216 nm diameter particles were pushed into a plane of symmetry running along the top of the electrodes and perpendicular to the surface, a region which corresponds to a minimum in the electric field. The fluid moved upward along this plane perpendicular to the surface, but the particles remained at the minimum on the electrode surface due to a combination of gravity, positive DEP and/or the presence of a stagnation point. The particle movement is shown schematically in figure 2, position B. The collection point in the centre of the electrodes was stable and it was observed that the 216 nm diameter spheres remained here for as long as the field was applied. At the same time the 93 nm spheres remained trapped at the electrode tips, under positive DEP forces, so that the two particle types were physically separated. The schematic separation shown in figure 2 is shown as a captured video image of a typical experiment in figure 3. The image was taken a few seconds after applying the 100 kHz field at 10 V peak to peak and shows the complete separation of the mixture into two bands. The 216 nm spheres fluoresce red and can be seen lined up along the symmetry axis of the electrodes, while the 93 nm spheres (green/yellow) remain at the electrode edges under a positive dielectrophoretic force. In this photograph these spheres can be seen forming long pearl chains extending from one electrode tip to the opposite neighbour. When the electric field was removed the particles rapidly dispersed into the medium.

The DEP force (equation (5)) depends on the volume whereas the Stoke's force (equation (6)) depends only on the radius. As a consequence, although the 93 nm diameter spheres experience a smaller viscous force than the 216 nm diameter spheres (approximately 2.3 times), they will also experience a much smaller DEP force (by a factor of 12.5). This implies that the smaller particles should move preferentially under the influence of viscous drag rather than the larger beads, contrary to our observations.

These observations can be explained by considering the magnitude of the Clausius–Mossotti factor (equation (4)) for the two spheres. The conductivity of a latex particle is given by the sum of the bulk conductivity and the surface conductivity, $\sigma_p = \sigma_b + (2K_s/a)$, where K_s is the surface conductance, σ_b the bulk conductivity (approximately zero for latex) and a the particle radius [12–14]. The surface conductance for the particle was obtained by measuring the frequency at which the force on the particle goes to zero, i.e. the frequency at which $\mathrm{Re}\{K(\omega)\} = 0$. For the 93 nm particles the value of K_s has been obtained

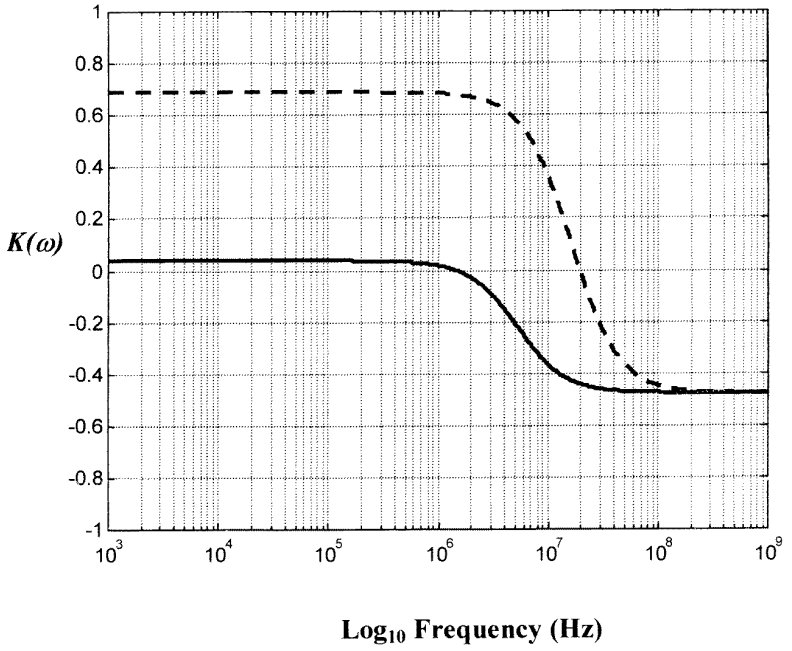

Figure 4. A Clausius–Mossotti plot showing the variation in the polarizability of the two types of beads as a function of frequency: full curve 216 nm beads; broken curve, 93 nm diameter beads. The plot was computed from equation (4) with K_s = 2.64 nS for the 93 nm diameter spheres and K_s = 0.9 nS for the 216 nm spheres and at a medium conductivity of 15 mS m^{-1}. At frequencies below 1 MHz both particles experience positive DEP, but the polarizability is much greater for the 93 nm particles so that the force is approximately 20 times greater than for the 216 nm particles.

previously [10] and is $K_s = 2.64$ nS. Measurements of the frequency at which the force is zero for the 216 nm particles were made in 0.1 mM KCl ($\sigma_m = 1.5$ mS^{-1}), and this frequency was found to be 3 ± 0.5 MHz. Assuming the particle permittivity, $\varepsilon_p = 2.5$, then the surface conductance was calculated as $K_s = 0.9$ nS. Using these data a plot of the frequency variation of the Clausius–Mossotti factor (equation (4)) for both the 93 nm and the 216 nm diameter particles was generated, and this is shown in figure 4. It is clear from the plot that at low frequencies (< 1 MHz) both particles experience positive DEP forces, but the magnitude of the Clausius–Mossotti factor for the 93 nm particle is approximately 20 times larger than for the 216 nm particle. Allowing for the difference in particle volumes, this means that the DEP force on the 93 nm particle is 1.6 times greater than on the 216 nm particle over a wide range of frequencies up to 1 MHz. However, to a first approximation and for a constant fluid velocity the viscous drag force on the 93 nm particles is 2.3 times smaller than on the 216 nm. The net balance of forces therefore is such that the larger particles move away from the electrode edges under the influence of EHD forces and are separated out from the smaller particles that remain trapped under dominant positive DEP forces.

We have previously shown that the latex spheres exhibit a distribution in surface charge density [10], which implies that the force on the beads will vary around a mean value. The Clausius–Mossotti plot shown in figure 4 should be taken to represent the mean values for the two particle sizes. This implies a spread in the magnitude of the DEP force on the particles. In our experiments no 216 nm spheres could be detected in the separated 93 nm population, indicating that the spread in surface charge on these spheres was small enough to make the ratio of DEP force to drag force always less than one.

In conclusion it has been demonstrated that the physical separation of two types of submicrometre particles can be achieved using a combination of DEP and EHD forces. The beads are spatially separated in the microelectrode array in a predictable manner. In combination with other separation techniques, based exclusively on the dielectric properties of particles [10], it should therefore be possible to spatially separate a heterogeneous mixture comprising a wide range of submicrometre particles into constituent particle types. This technology could have major advantages for processing and analysing small numbers of particles entirely 'on chip'.

The authors wish to acknowledge the UK Engineering and Physical Sciences Research Council for the award of a studentship to N G Green. This work was supported by the UK Biotechnology and Biological Sciences Research Council grant no 17/T05315.

References

[1] Pohl H A 1978 *Dielectrophoresis* (Cambridge: Cambridge University Press)
[2] Pethig R 1996 *Crit. Rev. Biotechnol.* **16** 331–48
[3] Becker F F, Wang X-B, Huang Y, Pethig R, Vykoukal J and Gascoyne P R C 1995 *Proc. Natl Acad. Sci. USA* **92** 860–4

[4] Müller T, Gerardino A, Schnelle T, Shirley S G, Bordoni F, De Gasperis G, Leoni R and Fuhr G 1996 *J. Phys. D: Appl. Phys.* **29** 340–9
[5] Washizu M, Suzuki S, Kurosawa O, Nishizaka T and Shinohara T 1994 *IEEE Trans. Ind. Appl.* **30** 835–43
[6] Morgan H and Green N G 1997 *J. Electrostatics* **35** 89–102
[7] Schnelle T, Müller T, Fiedler S, Shirley S G, Ludwig K, Hermann A, Fuhr G, Wagner B and Zimmerman U 1996 *Naturwissenschaften* **83** 172–6
[8] Müller T, Fiedler S, Schnelle T, Ludwig K, Jung H and Fuhr G 1996 *Biotechnol. Tech.* **4** 221–6
[9] Green N G, Millner J J and Morgan H 1997 *J. Biochem Biophys. Methods* **35** 89–102
[10] Green N G and Morgan H 1997 *J. Phys. D: Appl. Phys.* **30** L41–L44
[11] Ramos A, Morgan H, Green N G and Castellanos A *J. Phys. D: Appl. Phys.* submitted
[12] Green N G and Morgan H 1997 *J. Phys. D: Appl. Phys.* **30** 2626–33
[13] O'Konski C T 1960 *J. Phys. Chem.* **64** 605–19
[14] Arnold W M, Schwan H P and Zimmerman U 1987 *J. Phys. Chem.* **91** 5093–8